SIR Meta Distribution for Spatiotemporal Cooperation in Poisson Cellular Networks

Xinlei Yu, Qimei Cui, *Senior Member, IEEE*, and Martin Haenggi, *Fellow, IEEE*

***Abstract*—The meta distribution provides more fine-grained information on the signal-to-interference ratio (SIR) compared to the SIR distribution at the typical user. This paper studies the SIR meta distribution in heterogeneous cellular networks (HCNs) for JT-DPB with two types of hybrid automatic repeat request (HARQ) techniques, where JT-DPB is a general scheme for base station cooperation that combines joint transmission (JT) and dynamic point blanking (DPB). This paper also considers two types of typical users—the general user and the worst-case user (the typical user located at the Voronoi vertex in a single-tier network). For Type-II HARQ, a simplified network model is proposed, which leads to a tractable and accurate approach for the SIR meta distribution analysis. Analytical results for Type-I HARQ and Type-II HARQ are presented.**

***Index Terms*—JT-DPB, CoMP, HARQ, meta distribution, link reliability, HetNets, Poisson point process, stochastic geometry.**

I. Introduction

A. Motivation

With the increasing demand for data rate in 5G and later, most interference management techniques are used to mitigate the inter-cell interference and enhance the cell-edge coverage for heterogeneous cellular networks (HCNs). Coordinated multipoint transmission/reception (CoMP) and hybrid automatic repeat request (HARQ) are two key techniques, which represent *spatial cooperation* and *temporal cooperation*, respectively. The goal of this paper is an improved understanding of these *spatiotemporal cooperation* techniques by applying the concept of the meta distribution, a recently introduced performance metric that provides fine-grained information on the signal-to-interference ratio (SIR).

B. Related Work

A key question in the analysis of wireless networks is how to characterize the interference accurately. Stochastic geometry plays an important role in addressing this question. Using the probability generating functional (PGFL) [1, Thm. 4.9], the interference in networks modeled using the Poisson point process (PPP) can be characterized statistically, and the SIR-based performance analysis becomes tractable. The meta distribution of the SIR was recently introduced in [2] as a refinement of the standard SIR distribution (or success probability). Several studies based on meta distribution have being carried out, such as for D2D networks [3]–[5], base station cooperation [6], physical layer security [7], [8], NOMA [9], [10], cell range expansion [11] etc. [5], [12] apply the concept of the meta distribution for energy and rate, not merely the SIR. [13] proposes a simple approach to approximate the SIR meta distribution for general non-Poisson HCNs by relating it to the SIR analysis for the PPP. Besides, two efficient calculation methods of the meta distribution are provided in [14], [15].

As one of the spatial cooperation strategies, downlink CoMP transmission includes joint transmission (JT), dynamic point selection (DPS), dynamic point blanking (DPB), and coordinated scheduling/beamforming (CS/CB) [16]. Some prior works have used stochastic geometry to model and analyze JT and/or DPB, while most of them focus on the standard success probability (SIR distribution) as the performance metric. [17] analyzes non-coherent JT in terms of the SINR distribution in a single-tier Poisson cellular network and studies the effect of imperfect CSI and intra-cluster scheduling on non-coherent JT. [18] uses a homogeneous PPP to model base stations (BSs) in cellular networks and provides explicit integral expressions for the success probability of the typical user with DPB, which is sometimes called inter-cell interference coordination (ICIC). The joint use of JT and DPB is mentioned in a 3GPP technical report [16], but there are only very few works on this topic [19]–[21]. A rigorous analysis for the combined scheme of JT and DPB (ICIC), i.e., JT-DPB, is carried out in [6], and the SIR meta distribution of the general and worst-case user with JT-DPB or DPS/DPB is calculated.

As an important error control method, HARQ is mainly classified into two categories: Type-I HARQ and Type-II HARQ [22]. For Type-I HARQ, unsuccessful received data is discarded by the user, while the received data from different (re)transmissions in Type-II HARQ are combined to attempt decoding. Several works use stochastic geometry to model and analyze HARQ. [23] studies the performance of Type-I HARQ in ad hoc networks with time-correlated interference, and the outage probability, delay-limited throughput, and mean transmission time are derived in closed forms. Maximum ratio combining (MRC) is a common method for Type-II HARQ to maximize the SIR at receivers. [24], [25] analyze the performace of MRC receivers with spatial interference correlation under Rayleigh fading and Nakagami fading, respectively. [26] analyzes the performance of two types of HARQ in HCNs in term of the success probability and delay-limited throughput, where temporally correlated interference, flexible cell association, and BS load are jointly considered.

As a combination of spatial and temporal cooperation, [27] analyzes the standard success probability in downlink het-

Manuscript date May 28, 2019.

This work was supported in part by the Beijing Natural Science Foundation under Grant L182038, in part by the 111 Project of China under Grant B16006, in part by the BUPT Excellent Ph.D. Students Foundation under Grant CX2018205, and in part by China Scholarship Council (CSC) under Grant 201806470026. *(Corresponding author: Qimei Cui.)*

Xinlei Yu and Qimei Cui are with the National Engineering Laboratory for Mobile Network Technologies, Beijing University of Posts and Telecommunications, Beijing, 100876, China (e-mail: xinleiyu@hotmail.com, cuiqimei@bupt.edu.cn).

Martin Haenggi is with the Dept. of Electrical Engineering, University of Notre Dame, IN, 46556, USA (e-mail: mhaenggi@nd.edu).

erogeneous cellular networks with spatiotemporal cooperation techniques including JT, base station silencing, the Alamouti space-time code, and two types of HARQ—independent attempts and chase combining. However, the meta distribution analysis of these combined schemes is an open problem.

C. Contributions and Paper Organization

In this paper, we focus on the SIR meta distribution in heterogeneous cellular networks for JT-DPB with two types of HARQ. JT-DPB is a general scheme for base station cooperation that combines JT and DPB.

The contributions of the paper are:

- A spatiotemporal cooperation strategy combining spatial cooperation (JT-DPB) and temporal cooperation (HARQ) is studied rigorously.
- Two types of HARQ including Type-I HARQ (independent attempts) and Type-II HARQ (chase combining) are analyzed and compared.
- We derive the b-th moment for the general and worst-case users with JT-DPB and Type-I HARQ and the general user with JT-DPB and Type-II HARQ using stochastic geometry. Then the meta distributions are obtained from the moments.
- For Type-II HARQ, we propose a simplified network model and give a tight upper bound for the moments, whose accuracy is verified by comparing with the simulation results of original network model. This simplified network model can be used to study other transmission techniques.
- We consider two types of typical users—the general user and the worst-case user, where the worst-case user is the typical user located at the Voronoi vertex in a single-tier network, i.e., the typical cell-corner user.

The remainder of the paper is organized as follows. Sec. II introduces the system model. Sec. III presents the analysis of Type-I HARQ. Sec. IV shows the analysis of Type-II HARQ based on a novel simplified model. Sec. V shows numerical results for both types of HARQ and verifies the accuracy of the proposed simplified model. Sec. VI concludes the paper.

II. System Model

A. Network Model and SIR

We consider a K-tier PPP HCN model where the BSs belonging to i-th tier are distributed in $\mathbb{R}^2$ according to a homogeneous PPP Φ_i with density λ_i and transmit power P_i, $i = 1, \ldots, K$. We focus on the typical user at the origin $(0,0) \in \mathbb{R}^2$. Letting $\Phi \triangleq \bigcup_{i=1}^{K} \Phi_i$, the cooperation set of the typical user is denoted by $\mathcal{C} \subset \Phi$, and n denotes the cardinality of $\mathcal{C}$. For JT-DPB as introduced in [6], there are $m \leq n$ BSs in the cooperation set with strongest average received power transmitting the same message to the typical user, where these BSs form a subset $\mathcal{O} \subseteq \mathcal{C}$. JT ($m = n$) and DPB ($m = 1$) are two special cases of JT-DPB.

Since most HCNs are interference-limited [6], noise is ignored. Due to the time scale of the transmissions, we assume the cooperation set $\mathcal{C}$ and its subset $\mathcal{O}$ does not change in each (re)transmission of HARQ, and the average path loss terms are also time-invariant. Considering the case of non-coherent JT, the SIR of the i-th (re)transmission with JT-DPB at the typical user is given by

$$\mathrm{SIR}_i = \frac{\left| \sum_{x \in \mathcal{O}} P_{\nu(x)}^{1/2} \|x\|^{-\alpha/2} h_{x,i} \right|^2}{\sum_{x \in \mathcal{C}^c} P_{\nu(x)} \|x\|^{-\alpha} |h_{x,i}|^2}, \tag{1}$$

where the numerator is the combined desired signal power from the unsilenced cooperating BSs and the denominator is the interference power from the non-cooperating BSs; $\nu(x)$ denotes the index of the network tier of the BS located at x, i.e., $\nu(x) = i$ if and only if $x \in \Phi_i$; $h_{x,i} \sim \mathcal{N}_{\mathbb{C}}(0,1)$ denotes the i.i.d. Rayleigh fading between the typical user at $(0,0)$ and the BS at x in time slot i; $\alpha > 2$ is the path loss exponent; $\mathcal{C}^c \triangleq \Phi \backslash \mathcal{C}$ denotes the non-cooperation (i.e., interfering) set.

B. General and Worst-Case Users

The general user is the (overall) typical user, assumed at $(0,0) \in \mathbb{R}^2$ in the K-tier HCN. Its cooperation set $\mathcal{C}$ consists of the n BSs with the strongest average received power, i.e.,

$$\mathcal{C} = \arg \max_{\{x_1, \ldots, x_n\} \subset \Phi} \sum_{i=1}^{n} \frac{P_{\nu(x_i)}}{\|x_i\|^{\alpha}}. \tag{2}$$

A Voronoi vertex is a location at equal distance from three BSs. A user located at a Voronoi vertex is called a worst-case user. It is natural that we restrict the size of the cooperation set to $n \in \{1, 2, 3\}$ since these users have three equidistant BSs. To analyze the performance, we condition a Voronoi vertex to be located at $(0,0)$ in Φ and place the typical worst-case user at this location. Hence the cooperation set $\mathcal{C}$ of this user is a subset of the three BSs that are all closest to $(0,0)$, i.e.,

$$\mathcal{C} \subseteq \{x_1, x_2, x_3\}, \tag{3}$$

with $D \triangleq \|x_1\| = \|x_2\| = \|x_3\|$, where x_i denotes the location of the i-th closest BS to $(0,0)$.

C. HARQ Model

As an important decoding method, we consider the following two categories of HARQ similar to the model in [27]:

- **Type-I HARQ (Independent Attempts)**: This is the simplest version of HARQ. The typical user discards the received data in the erroneous transmissions and attempts decoding only from the last retransmission [27]. Given a threshold θ and a maximum number of transmissions N, the conditional success probability given the BS point process Φ can be expressed as

$$P_{\mathrm{s}}(\theta) = 1 - \mathbb{P}\Big(\bigcap_{i=1}^{N} \{\mathrm{SIR}_i < \theta\} \mid \Phi \Big). \tag{4}$$

- **Type-II HARQ (Chase Combining)**: In Type-II HARQ schemes, the typical user combines the data from different (re)transmissions to attempt decoding. These schemes can be further divided into chase combining and incremental redundancy. In this paper, we focus on the chase combining scheme. After N (re)transmissions, the combined SIR

using maximum-ratio combining (MRC) at the typical user is $\sum_{i=1}^{N} \mathrm{SIR}_i$. The conditional success probability given the BS point process Φ can be expressed as

$$P_{\mathrm{s}}^{\mathrm{MRC}}(\theta) = \mathbb{P}\Big(\sum_{i=1}^{N} \mathrm{SIR}_i > \theta \mid \Phi \Big). \tag{5}$$

D. The SIR Meta Distribution and its Beta Approximation

The meta distribution is the complementary cumulative distribution function (CCDF) of the conditional success probability $P_{\mathrm{s}}(\theta)$. It is formally defined as [2]

$$\bar{F}(\theta, x) \triangleq \bar{F}_{P_{\mathrm{s}}}(\theta, x) = \mathbb{P}(P_{\mathrm{s}}(\theta) > x),\ x \in [0,1]\,. \tag{6}$$

Since there is no known way to calculate the exact meta distribution directly, we derive it via the moments $M_b(\theta) \triangleq \mathbb{E}(P_{\mathrm{s}}(\theta)^b)$. One approach is to obtain a piecewise approximation [14] based on binomial mixtures from the integer moments $M_b = \mathbb{E}(P_{\mathrm{s}}(\theta)^b)$, $b \in \{0\} \cup \mathbb{N}$, as

$$\bar{F}_{P_{\mathrm{s}}}(x) = 1 - \lim_{i \to \infty} \sum_{k=0}^{\lfloor ix \rfloor} \sum_{j=k}^{i} \binom{i}{j} \binom{j}{k} (-1)^{j-k} M_j,\ x \in (0,1]\,, \tag{7}$$

and $\bar{F}_{P_{\mathrm{s}}}(0) = 1$, where $\lfloor u \rfloor$ is the largest integer smaller than or equal to u.

It is noteworthy that the meta distribution is the distribution of the conditional success probability $P_{\mathrm{s}}(\theta)$, while the standard success probability captures only the mean of $P_{\mathrm{s}}(\theta)$, i.e., $p_{\mathrm{s}}(\theta) \equiv M_1(\theta)$.

Alternatively, it is natural and often sufficient to approximate the meta distribution by matching its first and second moments M_1 and M_2 to the beta distribution, resulting in

$$\bar{F}_{P_{\mathrm{s}}}(x) \approx 1 - I_x\Big(\frac{M_1 \beta}{1 - M_1}, \beta\Big), \tag{8}$$

where

$$I_x(a,b) = \frac{\int_0^x t^{a-1}(1-t)^{b-1} \mathrm{d}t}{B(a,b)}, \tag{9}$$

$$\beta = \frac{(M_1 - M_2)(1 - M_1)}{M_2 - M_1^2}, \tag{10}$$

and $I_x(a,b)$ is the CDF of the beta distribution, i.e., the regularized incomplete beta function with shape parameters $a, b > 0$, and $B(a,b)$ is the beta function. This approximation has been shown to be rather accurate [2], [6].

III. Type-I HARQ

For $j \in [K]$, let $\Xi_j = \{\|x\|^\alpha / P_j,\ x \in \Phi_j\}$. According to the mapping theorem [1, Thm. 2.34] and the superposition property [1, Sec. 2.5] of the PPP, $\Xi = \bigcup_{j=1}^{K} \Xi_j$ is a non-homogeneous PPP on $\mathbb{R}^+$ with intensity function

$$\lambda(x) = \sum_{j=1}^{K} \lambda_j \pi \delta P_j^{\delta} x^{\delta - 1},\ x \in \mathbb{R}^+, \tag{11}$$

where $\delta = 2/\alpha$. We define the normalized path loss

$$\gamma_k = \|x_k\|^\alpha \,/ P_{\nu(x_k)} \tag{12}$$

as the k-th element in the ascending ordered set Ξ. The SIR of the i-th (re)transmission to the general user with JT-DPB can then be expressed as

$$\mathrm{SIR}_i^{\mathrm{g}} = \frac{\Big|\sum_{k=1}^{m} h_{x_k,i} \gamma_k^{-1/2}\Big|^2}{\sum_{k=n+1}^{\infty} \gamma_k^{-1} g_{k,i}}, \tag{13}$$

where $g_{k,i} = |h_{x_k,i}|^2$ and $m \le n$.

Similarly, for $n = 1, 2, 3$, the SIR of the i-th (re)transmission to the worst-case user with JT-DPB is

$$\mathrm{SIR}_i^{\mathrm{w}} = \frac{\Big|\sum_{k=1}^{m} D^{-\alpha/2} h_{x_k,i}\Big|^2}{\sum_{k=n+1}^{3} D^{-\alpha} g_{k,i} + \sum_{k=4}^{\infty} \|x_k\|^{-\alpha} g_{k,i}}, \tag{14}$$

where $m \le n$.

It is apparent from (13) and (14) that the SIRs of each (re)transmission are correlated due to the time-invariance of the average path loss terms.

Theorem 1 (Moments of $P_{\mathrm{s}}(\theta)$ for the general user with JT-DPB and Type-I HARQ) *The b-th moment $M_{b,N}$ of the conditional success probability $P_{\mathrm{s}}(\theta)$ for the general user in downlink cellular networks with JT-DPB and Type-I HARQ is*

$$M_{b,N} = \sum_{i=0}^{b} \sum_{j=0}^{iN} \binom{b}{i} \binom{iN}{j} (-1)^{i+j} T_j,\ b \in \mathbb{N}, \tag{15}$$

where

$$T_j = \int_{\substack{0 < u_1 < \cdots \\ \cdots < u_n < \infty}} \exp\left(-u_n\ {}_2F_1\left(j, -\delta; 1-\delta; \frac{-\theta}{\sum_{i=1}^{m} \big(\frac{u_n}{u_i}\big)^{\frac{1}{\delta}}} \right) \right) \mathrm{d}\mathbf{u}, \tag{16}$$

$\delta = 2/\alpha$, $\mathbf{u} = (u_1, u_2, \ldots, u_n)$, and ${}_2F_1(\cdot)$ is the Gaussian hypergeometric function.

Proof: According to (4), for Type-I HARQ, the conditional success probability $P_{\mathrm{s}}(\theta)$ for the general user with JT-DPB is given by

$$P_{\mathrm{s}}(\theta) = 1 - \mathbb{P}\Big(\bigcap_{i=1}^{N} \{\mathrm{SIR}_i^{\mathrm{g}} < \theta\} \mid \Xi \Big). \tag{17}$$

Given the point process Ξ, $\mathrm{SIR}_i^{\mathrm{g}}\,(i = 1, \ldots, N)$ are independent. Hence (17) can be written as

$$\begin{aligned} P_{\mathrm{s}}(\theta) &= 1 - \prod_{i=1}^{N} \mathbb{P}(\mathrm{SIR}_i^{\mathrm{g}} < \theta \mid \Xi) \\ &\overset{(a)}{=} 1 - \left(1 - \prod_{k=n+1}^{\infty} \frac{1}{1 + \theta G_m \gamma_k^{-1}}\right)^N, \end{aligned} \tag{18}$$

where (a) uses [6, Lemma 1] and $G_m \triangleq 1/\sum_{i=1}^{m} \gamma_i^{-1}$.

The b-th moments of $P_{\mathrm{s}}\,(\theta)$ can be expressed as

$$\begin{aligned} M_{b,N} &= \mathbb{E}\left(\left(1 - \left(1 - \prod_{k=n+1}^{\infty} \frac{1}{1 + \theta G_m \gamma_k^{-1}}\right)^N\right)^b \right) \\ &\overset{(a)}{=} \mathbb{E}\Bigg(\sum_{i=0}^{b} \binom{b}{i} (-1)^i \sum_{j=0}^{iN} \binom{iN}{j} \\ &\qquad \cdot (-1)^j \left(\prod_{k=n+1}^{\infty} \frac{1}{1 + \theta G_m \gamma_k^{-1}} \right)^j \Bigg) \end{aligned}$$

$$= \sum_{i=0}^{b} \sum_{j=0}^{iN} \binom{b}{i} \binom{iN}{j} \cdot (-1)^{i+j} \underbrace{\mathbb{E}\Big(\prod_{k=n+1}^{\infty} \left(\frac{1}{1+\theta G_m \gamma_k^{-1}} \right)^j \Big)}_{T_j}, \quad (19)$$

where (a) follows from the binomial theorem. From [6, Thm. 1], the term T_j in (19) can be expressed as (16). ■

Remark 1: The first moment $M_{1,N}$ for Type-I HARQ with no cooperation ($n = 1$) and arbitrary N was previously calculated in [18, Cor. 1].

Theorem 2 (Moments of $P_{\mathrm{s}}(\theta)$ for the worst-case user with JT-DPB) *For $n = 1, 2, 3$, the b-th moment $M_{b,N}$ of the conditional success probability $P_{\mathrm{s}}(\theta)$ for the worst-case user in downlink cellular networks with JT-DPB is given by*

$$M_{b,N} = \sum_{i=0}^{b} \sum_{j=0}^{iN} \binom{b}{i} \binom{iN}{j} (-1)^{i+j} T_j', \ b \in \mathbb{N}, \quad (20)$$

where

$$T_j' = \frac{\left(1+\frac{\theta}{m}\right)^{(n-3)j}}{\left({}_2F_1(j, -\delta; 1-\delta; -\frac{\theta}{m})\right)^2}, \quad (21)$$

$\delta = 2/\alpha$, and ${}_2F_1(\cdot)$ is the Gaussian hypergeometric function.

Proof: Similar to (18), the conditional success probability $P_{\mathrm{s}}(\theta)$ for the worst-case user in downlink cellular networks with JT-DPB and Type-I HARQ is

$$P_{\mathrm{s}}(\theta) = 1 - \prod_{i=1}^{N} \mathbb{P}(\mathrm{SIR}_i^{\mathrm{w}} < \theta \mid \Phi) \overset{(a)}{=} 1 - \left(1 - \left(1+\frac{\theta}{m}\right)^{n-3} \prod_{k=4}^{\infty} \frac{1}{1+\frac{\theta G_m}{\|x_k\|^\alpha}}\right)^N,$$

where (a) uses [6, Lemma 2] and $G_m \triangleq \frac{1}{mD^{-\alpha}}$.

The b-th moments of $P_{\mathrm{s}}(\theta)$ are derived as

$$\begin{aligned} M_{b,N} &= \mathbb{E}\left(\left(1 - \left(1 - \left(1+\frac{\theta}{m}\right)^{n-3} \prod_{k=4}^{\infty} \frac{1}{1+\frac{\theta G_m}{\|x_k\|^\alpha}}\right)^N\right)^b\right) \\ &\overset{(a)}{=} \mathbb{E}\left(\sum_{i=0}^{b} \binom{b}{i} (-1)^i \sum_{j=0}^{iN} \binom{iN}{j} (-1)^j \cdot \left(\left(1+\frac{\theta}{m}\right)^{n-3} \prod_{k=4}^{\infty} \frac{1}{1+\frac{\theta G_m}{\|x_k\|^\alpha}}\right)^j \right) \\ &= \sum_{i=0}^{b} \sum_{j=0}^{iN} \binom{b}{i} \binom{iN}{j} \cdot (-1)^{i+j} \underbrace{\mathbb{E}\left(\left(1+\frac{\theta}{m}\right)^{(n-3)j} \prod_{k=4}^{\infty} \left(\frac{1}{1+\frac{\theta G_m}{\|x_k\|^\alpha}}\right)^j \right)}_{T_j'}, \end{aligned} \quad (22)$$

where (a) follows from the binomial theorem. The term T_j' in (22) follows from [6, Thm. 2] as

$$T_j' = \int_0^\infty u \left(1+\frac{\theta}{m}\right)^{(n-3)j} \cdot \exp\left(-u \ {}_2F_1\left(j, -\delta; 1-\delta; -\frac{\theta}{m}\right)\right) \mathrm{d}u. \quad (23)$$

Since $j \in \mathbb{N}$, (23) can be simplified to (21) by using integration by parts. ■

IV. Type-II HARQ

A. Simplified Network Model

Here we give the formal definition for a simplified network in order to provide a tractable approach for the analysis of Type-II HARQ.

Before defining the simplified network model, we re-write the SIR as

$$\mathrm{SIR}(\Xi) = \frac{S(\Xi_1^n)}{I_1(\gamma_{n+1}) + I^!(\Xi_{n+2}^\infty)}, \quad (24)$$

where $\Xi_i^j = (\gamma_i, \ldots, \gamma_j)$. This representation highlights that the signal power is a function of the first n elements of Ξ and decomposes the interference into the contribution from the strongest interferer, denoted by I_1, and the rest of the interference, denoted by $I^!$.

Definition 1 (Simplified network model) *In the simplified network model, the interference $I^!(\Xi_{n+2}^\infty)$ is replaced by the interference of a virtual transmitter of received power $\mathbb{E}(I^!(\Xi_{n+2}^\infty) \mid \gamma_{n+1})$. The resulting SIR is*

$$\widetilde{\mathrm{SIR}}(\Xi) = \frac{S(\Xi_1^n)}{I_1(\gamma_{n+1}) + \mathbb{E}(I^!(\Xi_{n+2}^\infty) \mid \gamma_{n+1})}. \quad (25)$$

The substitution of the actual interference $I^!$ by its conditional mean is motivated by the fact that the variance of the interference outside a disk of a certain radius r tends to zero as r grows. To see this, let us calculate the variance of the interference $I = \sum_{k=n+1}^\infty \gamma_k^{-1} g_{k,i}$ outside of a normalized path loss l_0 by applying [1, Cor. 4.8]. Let $\psi(x) = \min\{l_0^{-1}, x^{-1}\}$ for $l_0 > 0$. For the PPP Ξ on $\mathbb{R}^+$, we have

$$\begin{aligned} \mathrm{var}\, I &= \int_{\mathbb{R}^+} \psi^2(x) \Lambda(\mathrm{d}x) \\ &= \int_{\mathbb{R}^+} \psi^2(x) \lambda(x) \mathrm{d}x \\ &= \int_0^{l_0} l_0^{-2} c x^{\delta-1} \mathrm{d}x + \int_{l_0}^\infty x^{-2} c x^{\delta-1} \mathrm{d}x \\ &= \pi \Big(\sum\nolimits_{j=1}^K \lambda_j P_j^\delta \Big) l_0^{-2+\frac{2}{\alpha}} \frac{2\alpha}{2\alpha-2}, \ \alpha > 1. \end{aligned} \quad (26)$$

According to (12), the normalized path loss l_0 and the radius r_0 follow the relation $l_0 \sim r_0^\alpha$. Hence, the variance goes to zero with $\Theta(r_0^{2-2\alpha})$. For $\alpha = 4$, this is $\Theta(r_0^{-6})$, which is indeed very fast.

B. SIR Analysis in the Simplified Model

Based on the simplified network model, the SIR of the i-th (re)transmission to the general user with JT-DPB and Type-II HARQ can be expressed as

$$\widetilde{\mathrm{SIR}}_i^{\mathrm{g}} = \frac{\left|\sum_{k=1}^{m} h_{x_k,i}\gamma_k^{-1/2}\right|^2}{\gamma_{n+1}^{-1}g_{n+1,i} + \mathbb{E}_{\boldsymbol{\gamma},g}\left(\sum_{k=n+2}^{\infty}\gamma_k^{-1}g_{k,i} \mid \gamma_{n+1}\right)}. \quad (27)$$

Given γ_{n+1}, since $g_{k,i} = |h_{x_k,i}|^2$ are i.i.d. exponential with unit mean, we have

$$\begin{aligned}
&\mathbb{E}_{\boldsymbol{\gamma},g}\left(\sum_{k=n+2}^{\infty}\gamma_k^{-1}g_{k,i} \mid \gamma_{n+1}\right) \\
&\quad= \mathbb{E}_{\boldsymbol{\gamma}}\left(\sum_{k=n+2}^{\infty}\gamma_k^{-1}\mathbb{E}_{\boldsymbol{g}}(g_{k,i}) \mid \gamma_{n+1}\right) \\
&\quad= \mathbb{E}_{\boldsymbol{\gamma}}\left(\sum_{k=n+2}^{\infty}\gamma_k^{-1} \mid \gamma_{n+1}\right) \\
&\quad\overset{(a)}{=} \int_{\gamma_{n+1}}^{\infty} x^{-1}\lambda(x)\mathrm{d}x \\
&\quad= \frac{c\gamma_{n+1}^{\delta-1}}{1-\delta}, \quad (28)
\end{aligned}$$

where (a) follows from Campbell's theorem for sums [1, Thm. 4.1], and the intensity function $\lambda(x)$ of Ξ is given in (11), and

$$c = \sum\nolimits_{j=1}^{K}\lambda_j\pi\delta P_j^{\delta}. \quad (29)$$

Hence, the SIR of the i-th (re)transmission to the general user with JT-DPB and Type-II HARQ is

$$\widetilde{\mathrm{SIR}}_i^{\mathrm{g}} = \frac{\left|\sum_{k=1}^{m} h_{x_k,i}\gamma_k^{-1/2}\right|^2}{\gamma_{n+1}^{-1}g_{n+1,i} + \gamma_{n+1}^{-1}\frac{c\gamma_{n+1}^{\delta}}{1-\delta}}. \quad (30)$$

C. Moments

In this paper, we restrict ourselves to the case of $N = 2$ (re)transmissions for Type-II HARQ. Its moments are given as follows.

Theorem 3 (Moments of $P_{\mathrm{s}}(\theta)$ for the general user with JT-DPB and Type-II HARQ) *In the simplified model, the b-th moment $\tilde{M}_b^{MRC}$ of the conditional success probability $P_{\mathrm{s}}(\theta)$ for the general user in downlink cellular networks with JT-DPB and Type-II HARQ is*

$$\begin{aligned}
\tilde{M}_b^{MRC} = &\int_{\substack{0<u_1<\cdots \\ \cdots<u_n<u_{n+1}<\infty}} \exp\left(-b\theta\frac{U_1}{U_2}\right)\exp(-u_{n+1}) \\
&\cdot\left(\frac{2}{2+\frac{\theta}{U_2}} + \frac{2\left(1+2U_1+\theta\frac{U_1}{U_2}\right)\ln\left(1+\frac{\theta}{U_2}\right)}{\left(2+\frac{\theta}{U_2}\right)^2}\right)^b \mathrm{d}\tilde{\mathbf{u}}, \quad (31)
\end{aligned}$$

where $\tilde{\mathbf{u}} = (u_1, u_2, \ldots, u_n, u_{n+1})$, and $U_1 = \frac{\delta}{1-\delta}u_{n+1}$, $U_2 = \sum_{i=1}^{m}\left(\frac{u_{n+1}}{u_i}\right)^{\frac{1}{\delta}}$.

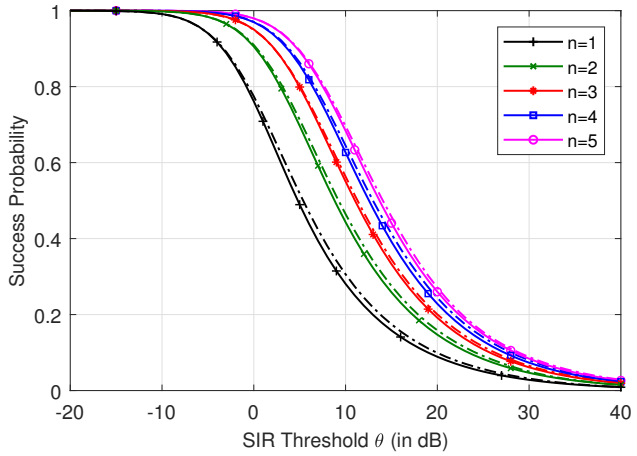

(a) Success probability

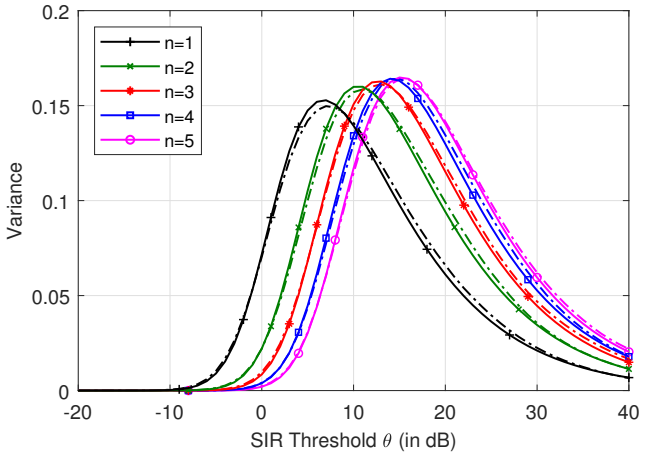

(b) Variance

Fig. 1. Success probability and variance of the general user with Type-II HARQ and JT for $\alpha = 4$. The solid lines are calculated from (33), and the dashed lines show the simulation results for Type-II HARQ.

Proof: Please see the Appendix. ■

Remark 2: Let $\mathrm{SIR}_i^{\mathrm{g}} \triangleq \frac{S}{I_1+I^!}$, and $\widetilde{\mathrm{SIR}}_i^{\mathrm{g}} \triangleq \frac{S}{I_1+\mathbb{E}(I^!)}$. Given S, I_1, since $\varphi(x) = \frac{S}{I_1+x}$, $x \in (0,+\infty)$, $S \geq 0, I_1 \geq 0$ is a convex function, according to Jensen's inequality [28, Thm. 1.6.2], we have $\varphi(\mathbb{E}(I^!)) \leq \mathbb{E}(\varphi(I^!))$, i.e., $\mathbb{E}(\widetilde{\mathrm{SIR}}_i^{\mathrm{g}}) \leq \mathbb{E}(\mathrm{SIR}_i^{\mathrm{g}})$. Hence, we can conjecture that the b-th moment $\tilde{M}_b^{\mathrm{MRC}}$ calculated by (33) based on the simplified network model is an upper bound of the actual moment M_b^{MRC}, i.e., $\tilde{M}_b^{\mathrm{MRC}} \geq M_b^{\mathrm{MRC}}$.

V. Numerical Results

Here we illustrate the analytical and simulated results for both types of HARQ. Fig. 1 and Fig. 2 show the accuracy of the approximated results for the general user with JT-DPB and Type-II HARQ calculated by (33), compared with their simulation results. Theorem 3 and the meta distribution derived from it provide very tight upper bounds for the actual values. It is noteworthy that the larger n, the better the approximation. The reason for this is that for larger n, the interference powers

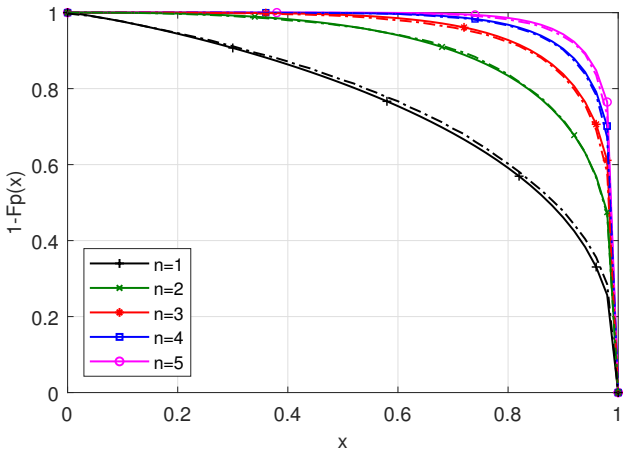

Fig. 2. SIR meta distribution of the general user with Type-II HARQ and JT for $\alpha = 4$, $\theta = 0$ dB. The solid lines are calculated from (33), and the dashed lines is the simulation results for Type-II HARQ.

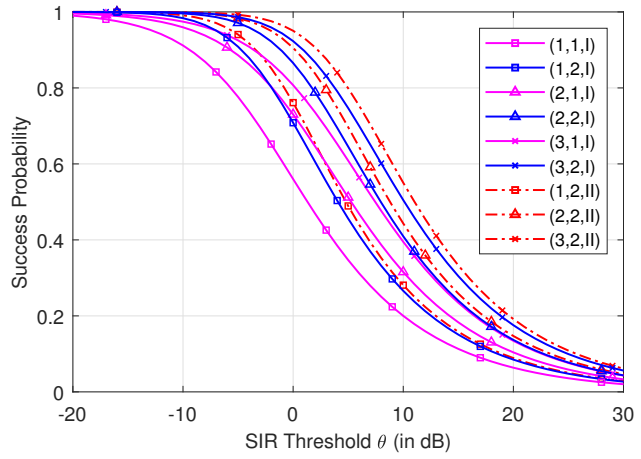

(a) General User

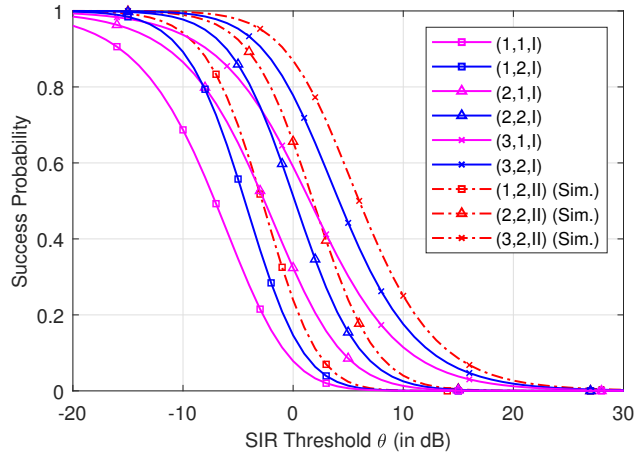

(b) Worst-case User

Fig. 3. Success probability of the general and worst-case user with JT and two types of HARQ for $\alpha = 4$. The triplet (n, N, type) is used for describing the curves in the legend of the figures. The results of Type-II HARQ for the worst-case user are simulated.

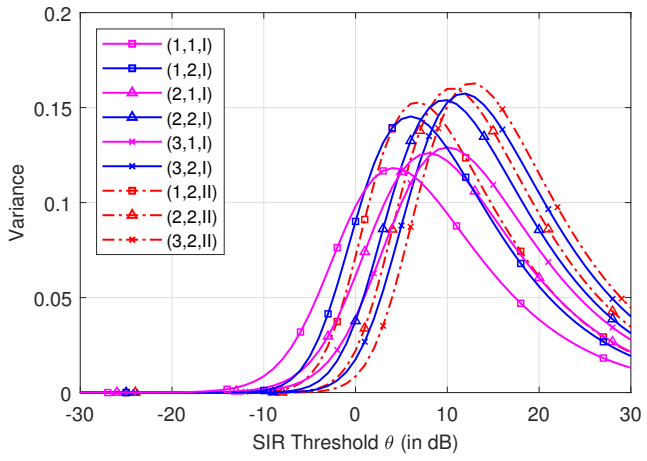

(a) General User

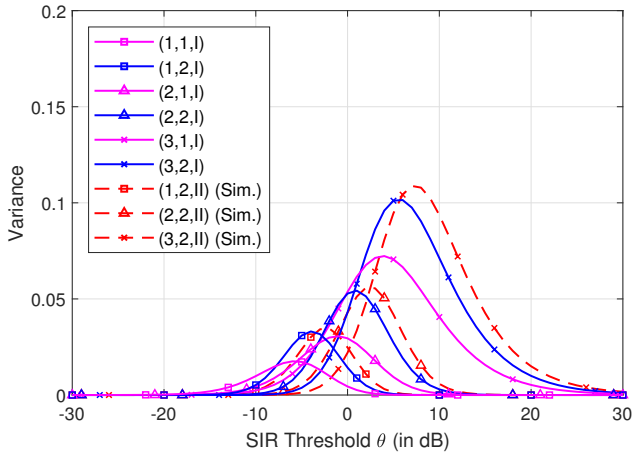

(b) Worst-case User

Fig. 4. Variance of the conditional success probability of the general and worst-case user with JT and two types of HARQ for $\alpha = 4$. The triplet (n, N, type) is used for describing the curves in the legend of the figures. The results of Type-II HARQ for the worst-case user are simulated.

from the individual BSs become more comparable and smaller, hence their sum is better approximated by the mean, see (26).

Fig. 3 and Fig. 4 show the success probability and variance of the two types of users with JT and HARQ, and Fig. 5 plots the beta approximation of the SIR meta distribution.

For the general user with Type-I HARQ and no cooperation ($n = 1$), Fig. 6 shows the reliability of the "10% user" with the SIR threshold $\theta = 0$ dB, i.e., the reliability x that 90% of the users achieve but 10% do not, and the success probability. The success probability indicates a very limited gain in increasing N from 9 to 10, while the 10% user performance reveals that there is still a noticeable benefit. Specifically, as N is changed from 9 to 10, the gains in the success probability and the meta distribution (in terms of x) are about 0.008 and 0.038, respectively.

Fig. 7 shows a comparison between the two HARQ techniques. It reveals that Type-I HARQ with $N = 3$ is very close to Type-II HARQ with $N = 2$.

Fig. 8 shows another important result for the tradeoff between spatial and temporal correlation for the general user

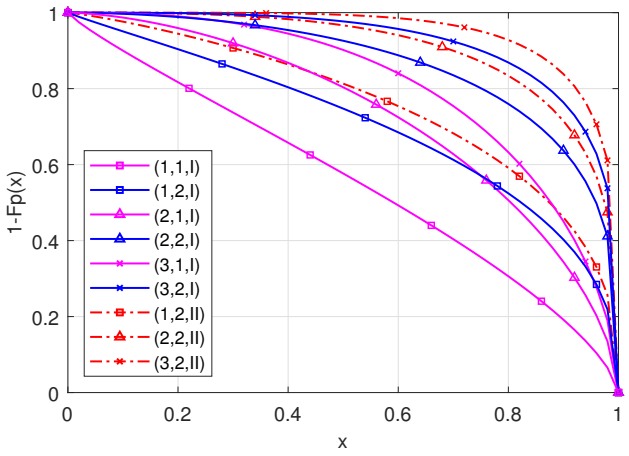

(a) General User

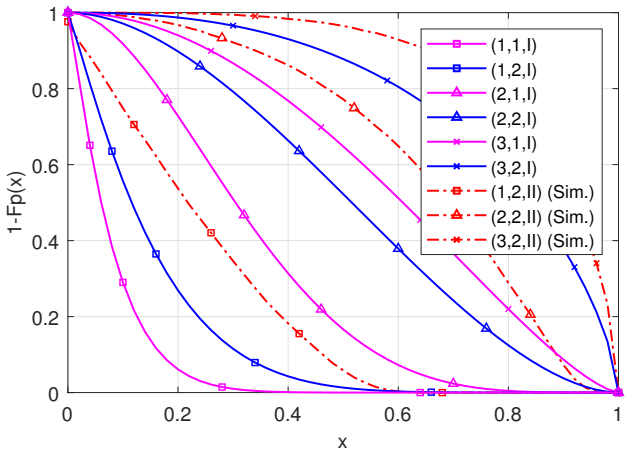

(b) Worst-case User

Fig. 5. SIR meta distribution of user with JT and two types of HARQ where $\theta = 0$ dB and $\alpha = 4$. The triplet (n, N, type) is used for describing the curves in the legend of the figures. The results of Type-II HARQ for the worst-case user are simulated.

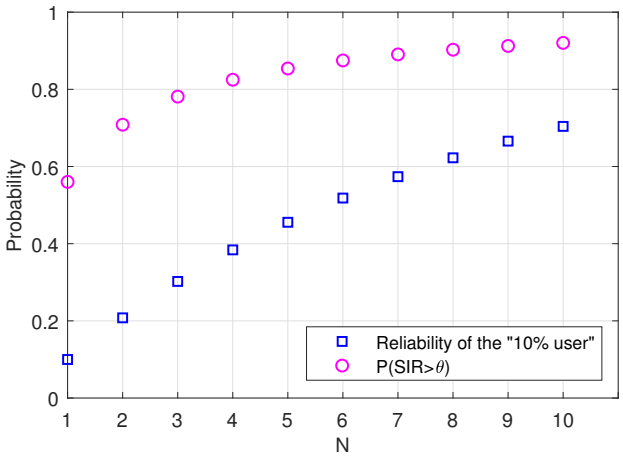

Fig. 6. (Mean) success probability and "10% user" reliability with the SIR thresold $\theta = 0$ dB for the general user with Type-I HARQ and no cooperation $(n = 1)$.

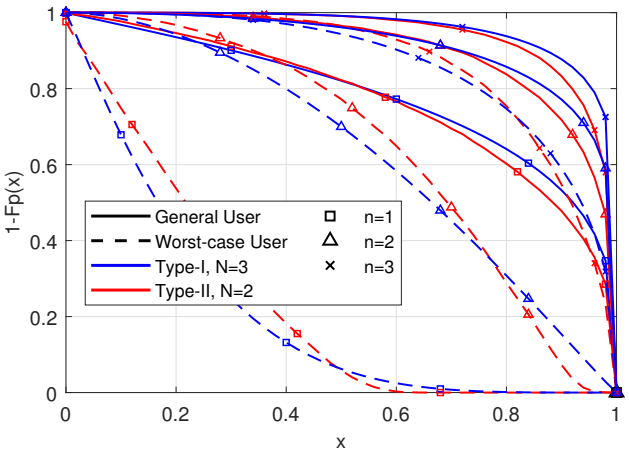

Fig. 7. Comparison of the meta distribution for $\theta = 0$ dB between Type-I HARQ with $N = 3$ and Type-II HARQ with $N = 2$. The results of the worst-case user with Type-II HARQ and JT are simulated.

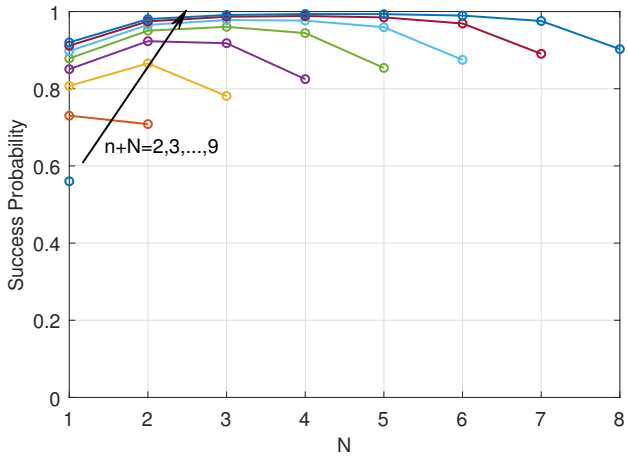

(a) Success probability

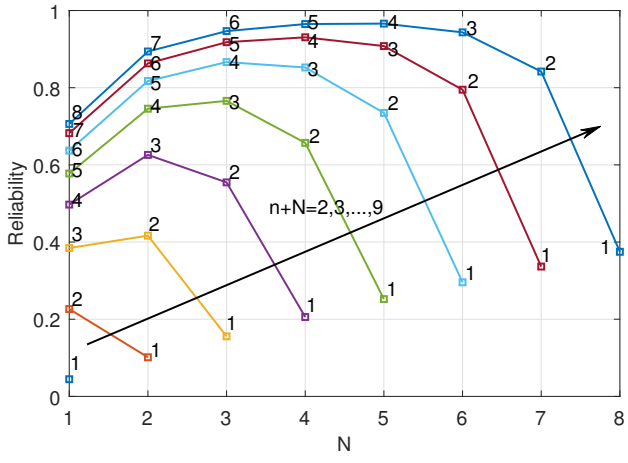

(b) "5% user" reliability

Fig. 8. (Mean) success probability and "5% user" reliability with the SIR thresold $\theta = 0$ dB for the general user with Type-I HARQ and JT, given the fixed $n + N$ from 2 to 9. Each line has a fixed $n + N$, and the digit near the markers is the cardinality n of the cooperation set $\mathcal{C}$.

with Type-I HARQ and JT. For a fixed $n+N$, the combination of (n, N) that gives the best performance can be determined, in terms of the mean success probability and in terms of the performance of the 5% user. As shown in Fig. 8(b), the combinations with the best performance for fixed $n+N$ are keeping a balance between spatial and temporal cooperation. For example, given $n+N=6$, the combination of (n, N) with the best performance is $(3, 3)$.

VI. Conclusion

In this paper, we study the SIR meta distribution in HCNs for JT-DPB with two classes of HARQ, which provides more fine-grained information than the standard success probability. For Type-I HARQ, the link reliability and the reliability of user percentiles are obtained analytically. The results reveal that the standard success probability does not capture the benefit to the user percentiles of increasing the number of transmissions, and the comparison with Type-II HARQ shows that Type-II HARQ achieves comparable performance with $N=2$ as Type-I HARQ with $N=3$. Besides, our results indicate that a balanced combination between spatial and temporal cooperation achieves the best performance. The future work includes the SIR meta distribution analysis of another type of HARQ—incremental redundancy HARQ (HARQ-IR), which is regarded as the most sophisticated HARQ since it retransmits redundancy bits rather than the same signal.

Appendix
Proof of Theorem 3

According to (5), given the point process Ξ, the conditional success probability $P_{\mathrm{s}}^{\mathrm{MRC}}(\theta)$ is

$$P_{\mathrm{s}}^{\mathrm{MRC}}(\theta)=\mathbb{P}(\widetilde{\mathrm{SIR}}_1^{\mathrm{g}}+\widetilde{\mathrm{SIR}}_2^{\mathrm{g}}>\theta\mid\Xi). \tag{32}$$

Given the point process Ξ, $\widetilde{\mathrm{SIR}}_1^{\mathrm{g}}$ and $\widetilde{\mathrm{SIR}}_2^{\mathrm{g}}$ are independent. Letting $Z=\widetilde{\mathrm{SIR}}_2^{\mathrm{g}}$, (34) can be written as

$$\begin{aligned}
P_{\mathrm{s}}^{\mathrm{MRC}}(\theta)&=\mathbb{P}(\widetilde{\mathrm{SIR}}_1^{\mathrm{g}}+Z>\theta\mid\Xi)\\
&=\mathbb{E}(\mathbb{P}(\widetilde{\mathrm{SIR}}_1^{\mathrm{g}}>\theta-Z\mid\Xi,Z))\\
&=\mathbb{E}\Bigg(\mathbb{P}\Bigg(\left|\sum_{k=1}^{m}h_{x_k,1}\gamma_k^{-1/2}\right|^2>(\theta-Z)\\
&\qquad\cdot\left(\gamma_{n+1}^{-1}g_{n+1,1}+\gamma_{n+1}^{\delta-1}\frac{c}{1-\delta}\right)\mid\Xi,Z\Bigg)\Bigg)\\
&\overset{(a)}{=}\mathbb{E}\Bigg(\exp\left(-\frac{(\theta-Z)^+\gamma_{n+1}^{-1}g_{n+1,1}}{\sum_{k=1}^{m}\gamma_k^{-1}}\right)\\
&\qquad\cdot\exp\left(-\frac{(\theta-Z)^+\gamma_{n+1}^{\delta-1}\frac{c}{1-\delta}}{\sum_{k=1}^{m}\gamma_k^{-1}}\right)\mid\Xi\Bigg)\\
&\overset{(b)}{=}\mathbb{E}_{Z|\Xi}\Bigg(\frac{1}{1+\frac{(\theta-Z)^+\gamma_{n+1}^{-1}}{\sum_{k=1}^{m}\gamma_k^{-1}}}\\
&\qquad\cdot\exp\left(-\frac{(\theta-Z)^+\gamma_{n+1}^{\delta-1}\frac{c}{1-\delta}}{\sum_{k=1}^{m}\gamma_k^{-1}}\right)\mid\Xi\Bigg)\\
&\overset{(c)}{=}\mathbb{E}_{Z|\Xi}\left(\frac{\exp(-s_2(\theta-Z)^+)}{1+s_1(\theta-Z)^+}\mid\Xi\right),
\end{aligned} \tag{33}$$

where (a) follows since $\left|\sum_{k=1}^{m}\gamma_k^{-1/2}h_{x_k,1}\right|^2$ is exponentially distributed with mean $\sum_{k=1}^{m}\gamma_k^{-1}$, (b) since $g_{n+1,1}=|h_{x_n+1,1}|^2$ is i.i.d. exponential with unit mean, and (c) is obtained by letting $s_1=\frac{\gamma_{n+1}^{-1}}{\sum_{k=1}^{m}\gamma_k^{-1}}$, and $s_2=\frac{\gamma_{n+1}^{\delta-1}\frac{c}{1-\delta}}{\sum_{k=1}^{m}\gamma_k^{-1}}$.

Then, the conditional CDF of Z can be obtained by

$$\begin{aligned}
\mathbb{P}(Z\le z\mid\Xi)&=1-\mathbb{P}(Z>z\mid\Xi)\\
&=1-\frac{\exp(-s_2z)}{1+s_1z},
\end{aligned} \tag{34}$$

and the conditional PDF of Z follows as

$$\begin{aligned}
f_{Z|\Xi}(z)&=\frac{\mathrm{d}\mathbb{P}(Z\le z\mid\Xi)}{\mathrm{d}z}\\
&=\frac{s_1\exp(-s_2z)}{(1+s_1z)^2}+\frac{s_2\exp(-s_2z)}{1+s_1z}.
\end{aligned} \tag{35}$$

Using this conditional PDF of Z, the expectation over Z in (35) can be computed as

$$\begin{aligned}
P_{\mathrm{s}}^{\mathrm{MRC}}(\theta)&=\mathbb{E}_{Z|\Xi}\left(\frac{\exp(-s_2(\theta-Z)^+)}{1+s_1(\theta-Z)^+}\mid\Xi\right)\\
&=\int_0^\infty\frac{\exp(-s_2(\theta-z)^+)}{1+s_1(\theta-z)^+}f_{Z|\Xi}(z)\mathrm{d}z\\
&=\int_0^\theta\frac{\exp(-s_2(\theta-z))}{1+s_1(\theta-z)}f_{Z|\Xi}(z)\mathrm{d}z+\int_\theta^\infty f_{Z|\Xi}(z)\mathrm{d}z\\
&=\exp(-s_2\theta)\Bigg(\frac{2}{2+s_1\theta}\\
&\qquad+\frac{2(s_1+2s_2+s_1s_2\theta)\ln(1+s_1\theta)}{s_1(2+s_1\theta)^2}\Bigg).
\end{aligned} \tag{36}$$

Hence, the b-th moments of $P_{\mathrm{s}}^{\mathrm{MRC}}(\theta)$ are derived as

$$\begin{aligned}
\tilde{M}_b^{\mathrm{MRC}}&=\mathbb{E}((P_{\mathrm{s}}^{\mathrm{MRC}}(\theta))^b)\\
&=\mathbb{E}\Bigg(\exp(-bs_2\theta)\Bigg(\frac{2}{2+s_1\theta}\\
&\qquad+\frac{2(s_1+2s_2+s_1s_2\theta)\ln(1+s_1\theta)}{s_1(2+s_1\theta)^2}\Bigg)^b\Bigg)\\
&=\int\limits_{\substack{0<r_1<\cdots\\ \cdots<r_n<r_{n+1}<\infty}}\exp(-bs_2\theta)\Bigg(\frac{2}{2+s_1\theta}\\
&\qquad+\frac{2(s_1+2s_2+s_1s_2\theta)\ln(1+s_1\theta)}{s_1(2+s_1\theta)^2}\Bigg)^b f_{\boldsymbol{\gamma}}(\mathbf{r})\mathrm{d}\mathbf{r}\\
&=\int\limits_{\substack{0<r_1<\cdots\\ \cdots<r_n<r_{n+1}<\infty}}\exp\left(-\frac{b\theta r_{n+1}^{\delta-1}\frac{c}{1-\delta}}{\sum\limits_{k=1}^{m}r_k^{-1}}\right)\Bigg(\frac{2}{2+\frac{\theta r_{n+1}^{-1}}{\sum\limits_{k=1}^{m}r_k^{-1}}}\\
&\quad+\frac{2\Big(1+2r_{n+1}^{\delta}\frac{c}{1-\delta}+\frac{\theta r_{n+1}^{\delta-1}\frac{c}{1-\delta}}{\sum\limits_{k=1}^{m}r_k^{-1}}\Big)\ln\Big(1+\frac{\theta r_{n+1}^{-1}}{\sum\limits_{k=1}^{m}r_k^{-1}}\Big)}{(2+\frac{\theta r_{n+1}^{-1}}{\sum\limits_{k=1}^{m}r_k^{-1}})^2}\Bigg)^b f_{\boldsymbol{\gamma}}(\mathbf{r})\mathrm{d}\mathbf{r},
\end{aligned} \tag{37}$$

where the joint PDF of $\boldsymbol{\gamma} = (\gamma_1, \gamma_2, \ldots, \gamma_n, \gamma_{n+1})$ is given by [6, eq. (15)], i.e., for $0 < \gamma_1 < \cdots < \gamma_n < \gamma_{n+1}$,

$$f_{\boldsymbol{\gamma}}(\boldsymbol{r}) = \left(\pi\delta \sum_{i=1}^{K} \lambda_i P_i^{\delta}\right)^{n+1} \cdot \exp\left(-\pi \sum_{i=1}^{K} \lambda_i P_i^{\delta} r_{n+1}^{\delta}\right) \prod_{i=1}^{n+1} r_i^{\delta-1}. \quad (38)$$

By changing the variables of this integration, i.e., letting $u_j = \pi \sum_{i=1}^{K} \lambda_i P_i^{\delta} r_j^{\delta}$, $j = 1, 2, \ldots, n+1$, (39) can be simplified to (33).

REFERENCES

[1] M. Haenggi, *Stochastic Geometry for Wireless Networks*. Cambridge University Press, 2012.

[2] ——, "The meta distribution of the SIR in Poisson bipolar and cellular networks," *IEEE Trans. Wireless Commun.*, vol. 15, pp. 2577–2589, Apr. 2016.

[3] M. Salehi, A. Mohammadi, and M. Haenggi, "Analysis of D2D underlaid cellular networks: SIR meta distribution and mean local delay," *IEEE Trans. Commun.*, vol. 65, pp. 2904–2916, Jul. 2017.

[4] N. Deng and M. Haenggi, "A fine-grained analysis of millimeter-wave device-to-device networks," *IEEE Trans. Commun.*, vol. 65, pp. 4940–4954, Nov. 2017.

[5] ——, "The energy and rate meta distributions in wirelessly powered D2D networks," *IEEE J. Sel. Areas Commun.*, vol. 37, pp. 269–282, Feb. 2019.

[6] Q. Cui, X. Yu, Y. Wang, and M. Haenggi, "The SIR meta distribution in Poisson cellular networks with base station cooperation," *IEEE Trans. Commun.*, vol. 66, pp. 1234–1249, Mar. 2018.

[7] Q. Cui, X. Jiang, X. Yu, Y. Wang, and M. Haenggi, "SIR meta distribution in physical layer security with interference correlation," in *Proc. IEEE Global Communications Conference (GLOBECOM)*, Dec. 2018, pp. 1–6.

[8] J. Tang, G. Chen, and J. P. Coon, "Meta distribution of the secrecy rate in the presence of randomly located eavesdroppers," *IEEE Wireless Commun. Lett.*, vol. 7, pp. 630–633, Aug. 2018.

[9] M. Salehi, H. Tabassum, and E. Hossain, "Meta distribution of SIR in large-scale uplink and downlink NOMA networks," *IEEE Trans. Commun.*, vol. 67, pp. 3009–3025, Apr. 2019.

[10] K. S. Ali, H. El. Sawy, and M.-S. Alouini, "Meta distribution of downlink non-orthogonal multiple access (NOMA) in Poisson networks," *IEEE Wireless Commun. Lett.*, vol. 8, pp. 572–575, Apr. 2019.

[11] Y. Wang, M. Haenggi, and Z. Tan, "SIR meta distribution of K-tier downlink heterogeneous cellular networks with cell range expansion," *IEEE Trans. Commun.*, vol. 67, pp. 3069–3081, Apr. 2019.

[12] N. Deng and M. Haenggi, "SINR and rate meta distributions for HCNs with joint spectrum allocation and offloading," *IEEE Trans. Commun.*, vol. 67, pp. 3709–3722, May 2019.

[13] S. S. Kalamkar and M. Haenggi, "Simple approximations of the SIR meta distribution in general cellular networks," *IEEE Trans. Commun.*, 2019, Accepted.

[14] M. Haenggi, "Efficient calculation of meta distributions and the performance of user percentiles," *IEEE Wireless Commun. Lett.*, vol. 7, pp. 982–985, Dec. 2018.

[15] S. Guruacharya and E. Hossain, "Approximation of meta distribution and its moments for Poisson cellular networks," *IEEE Wireless Commun. Lett.*, vol. 7, pp. 1074–1077, Dec. 2018.

[16] 3GPP, "Coordinated multi-point operation for LTE physical layer aspects," TR 36.819, Tech. Rep., Sep. 2013, available at http://www.3gpp.org/DynaReport/36819.htm.

[17] R. Tanbourgi, S. Singh, J. G. Andrews, and F. K. Jondral, "A tractable model for noncoherent joint-transmission base station cooperation," *IEEE Trans. Wireless Commun.*, vol. 13, pp. 4959–4973, Sep. 2014.

[18] X. Zhang and M. Haenggi, "A stochastic geometry analysis of inter-cell interference coordination and intra-cell diversity," *IEEE Trans. Wireless Commun.*, vol. 13, pp. 6655–6669, Dec. 2014.

[19] D. Marabissi, G. Bartoli, R. Fantacci, and M. Pucci, "An optimized CoMP transmission for a heterogeneous network using eICIC approach," *IEEE Trans. Veh. Technol.*, vol. 65, pp. 8230–8239, Oct. 2016.

[20] W. Zuo, H. Xia, and C. Feng, "A novel coordinated multi-point transmission in dense small cell deployment," in *Proc. 2015 IEEE 26th Annual International Symposium on Personal, Indoor, and Mobile Radio Communications (PIMRC)*, Aug. 2015, pp. 1872–1877.

[21] Y.-N. R. Li, J. Li, W. Li, Y. Xue, and H. Wu, "CoMP and interference coordination in heterogeneous network for LTE-advanced," in *Proc. IEEE GLOBECOM Workshops*, Dec. 2012, pp. 1107–1111.

[22] 3GPP, "Evolved universal terrestrial radio access (E-UTRA); radio resource control (RRC); protocol specification," TS 36.331, Tech. Rep., Mar. 2015, available at https://www.3gpp.org/ftp/Specs/2015-03/Rel-12/36_series/36331-c50.zip.

[23] H. Ding, S. Ma, C. Xing, Z. Fei, Y. Zhou, and C. L. P. Chen, "Analysis of hybrid ARQ in ad hoc networks with correlated interference and feedback errors," *IEEE Trans. Wireless Commun.*, vol. 12, pp. 3942–3955, Aug. 2013.

[24] R. Tanbourgi, H. S. Dhillon, J. G. Andrews, and F. K. Jondral, "Dual-branch MRC receivers under spatial interference correlation and Nakagami fading," *IEEE Trans. Commun.*, vol. 62, pp. 1830–1844, Jun. 2014.

[25] ——, "Effect of spatial interference correlation on the performance of maximum ratio combining," *IEEE Trans. Wireless Commun.*, vol. 13, pp. 3307–3316, Jun. 2014.

[26] M. Sheng, J. Wen, J. Li, B. Liang, and X. Wang, "Performance analysis of heterogeneous cellular networks with HARQ under correlated interference," *IEEE Trans. Wireless Commun.*, vol. 16, pp. 8377–8389, Dec. 2017.

[27] G. Nigam, P. Minero, and M. Haenggi, "Spatiotemporal cooperation in heterogeneous cellular networks," *IEEE J. Sel. Areas Commun.*, vol. 33, pp. 1253–1265, Jun. 2015.

[28] R. Durrett, *Probability: theory and examples*, 5th ed. Cambridge University Press, 2019.

Xinlei Yu received the B.S. degree in communication engineering from Southwest Jiaotong University (SWJTU), Chengdu, China, in 2015. He is currently pursuing the Ph.D. degree in information and communications engineering with the Beijing University of Posts and Telecommunications (BUPT), Beijing, China. From September 2018 to September 2019, he was a visiting Ph. D. student at the University of Notre Dame, Indiana, USA, under the supervision of Professor Martin Haenggi. His research interests are in the area of the modeling and analysis of cellular networks using stochastic geometry, with current emphasis on heterogeneous cellular networks, cooperation communication.

Qimei Cui (M'09-SM'15) received the B.E. and M.S. degrees in electronic engineering from Hunan University, Changsha, China, in 2000 and 2003, respectively, and the Ph.D. degree in information and communications engineering from the Beijing University of Posts and Telecommunications (BUPT), Beijing, China, in 2006. She has been a Full Professor with the School of Information and Communication Engineering, BUPT, since 2014. She was a Guest Professor with the Department of Electronic Engineering, University of Notre Dame, IN, USA, in 2016. Her main research interests include spectral-efficiency or energy-efficiency based transmission theory, and networking technology for 4G/5G broadband wireless communications and green communications. She serves as a Technical Program Committee Member for several international conferences, such as the IEEE ICC, the IEEE WCNC, the IEEE PIMRC, the IEEE ICCC, the IEEE ISCIT 2012, and the IEEE WCSP 2013. She was a recipient of the Honorable Mention Demo Award at the ACM MobiCom 2009, the Best Paper Award at the IEEE ISCIT 2012 and the IEEE WCNC 2014, and the Young Scientist Award at the URSI GASS 2014. She serves as a Guest Editor for the *EURASIP Journal on Wireless Communications and Networking*, *International Journal of Distributed Sensor Networks*, and *Journal of Computer Networks and Communications*.

Martin Haenggi (S'95-M'99-SM'04-F'14) received the Dipl.-Ing. (M.Sc.) and Dr.sc.techn. (Ph.D.) degrees in electrical engineering from the Swiss Federal Institute of Technology in Zurich (ETH) in 1995 and 1999, respectively. Currently he is the Freimann Professor of Electrical Engineering and a Concurrent Professor of Applied and Computational Mathematics and Statistics at the University of Notre Dame, Indiana, USA. In 2007-2008, he was a visiting professor at the University of California at San Diego, and in 2014-2015 he was an Invited Professor at EPFL, Switzerland.

He is a co-author of the monographs "Interference in Large Wireless Networks" (NOW Publishers, 2009) and "Stochastic Geometry Analysis of Cellular Networks" (Cambridge University Press, 2018) and the author of the textbook "Stochastic Geometry for Wireless Networks" (Cambridge, 2012), and he published 15 single-author journal articles. His scientific interests lie in networking and wireless communications, with an emphasis on cellular, amorphous, ad hoc (including D2D and M2M), cognitive, and vehicular networks.

He served as an Associate Editor of the Elsevier Journal of Ad Hoc Networks, the IEEE Transactions on Mobile Computing (TMC), the ACM Transactions on Sensor Networks, as a Guest Editor for the IEEE Journal on Selected Areas in Communications, the IEEE Transactions on Vehicular Technology, and the EURASIP Journal on Wireless Communications and Networking, as a Steering Committee member of the TMC, and as the Chair of the Executive Editorial Committee of the IEEE Transactions on Wireless Communications (TWC). From 2017 to 2018, he was the Editor-in-Chief of the TWC. He also served as a Distinguished Lecturer for the IEEE Circuits and Systems Society, as a TPC Co-chair of the Communication Theory Symposium of the 2012 IEEE International Conference on Communications (ICC'12), of the 2014 International Conference on Wireless Communications and Signal Processing (WCSP'14), and the 2016 International Symposium on Wireless Personal Multimedia Communications (WPMC'16).

For both his M.Sc. and Ph.D. theses, he was awarded the ETH medal. He also received a CAREER award from the U.S. National Science Foundation in 2005 and three awards from the IEEE Communications Society, the 2010 Best Tutorial Paper award, the 2017 Stephen O. Rice Prize paper award, and the 2017 Best Survey paper award, and he is a 2017 and 2018 Clarivate Analytics Highly Cited Researcher.